Journal of Marine Science and Application (2025) 24: 1230-1238
https://doi.org/10.1007/s11804-025-00670-2

RESEARCH ARTICLE

Experimental Investigation of Dual T-foil System on the Pitch Motion Reduction of a Monohull Vessel

Yichen Jiang[1], Shijie Liu[1], Junyu Bai[2], Zhi Zong[3] and Guiyong Zhang[1]

Received: 09 September 2024 / Accepted: 11 October 2024

Abstract

As a vessel navigates at high speeds in waves, considerable pitching motion can result in the discomfort of passengers. In this study is proposed a ride control system consisting of dual T-foils to generate a larger righting moment than a common single T-foil system. One T-foil is mounted at the bow, and the other at the stern. Accordingly, different control strategies for dual T-foils were proposed To verify the stratigies, a model experiment was conducted in the Towing Tank, Dalian Unievrsity of Technology. The optimal control signal was determined by comparing the pitch responses, heave responses, bow accelerations, and stern accelerations of a vessel in regular waves. In addition, the control strategy for the best motion-reduction effect was investigated. The optimized dual T-foil system provides a 34% reduction in pitch motion.

Keywords T-foil; Active control; High-speed vessel; Ride control system; Control strategy

1 Introduction

1.1 Background and relevant work

Considerable vertical motion responses can lead to decreased passenger comfort under adverse sea conditions (Davis and Hollway, 2003; Hollway and Davis, 2006). Ride control systems (RCSs), such as T-foils, fins, Hull Vanes, and stern spoilers, have been widely utilized to enhance seakeeping performance (Fang and Chan, 2007; Thomas et al., 2011; Jacobi et al., 2012; Liu et al., 2021; Gopinath and Vijayakumar, 2023). However, only an active control T-foil has been demonstrated as an effective solution for mitigating the motion responses of high-speed vessels.

Esteban et al. (2000) conducted a comprehensive numerical analysis of the active control of T-foil and confirmed that the effectiveness of motion reduction primarily relies on the control strategy implemented for the "Silvia Ana" fast ferry model equipped with a T-foil and two stern spoilers. Furthermore, experiments carried out on a deep-V monohull model demonstrate that the modular architecture of an active controller can incorporate analysis of various control strategies (Esteban et al., 2001). Given the dynamic characteristics of ships, ensuring that these actuators operate swiftly and efficiently is essential. Hence, several controller solutions have been proposed, including conventional PID, multivariable PID, multiobjective control strategy, and nonlinear control strategy (Giron-Sierra et al., 2001; Aranda et al., 2001; Esteban et al., 2002; Giron-Sierra et al., 2002). The ship actuator control model was developed using SIMULINK as an effective simulation environment focused on control aspects (Polo et al., 2001; Esteban et al., 2005).

The University of Tasmania has conducted a series of experimental studies on the motion-reduction performance of T-foils to confirm their reliability. AlaviMehr et al. (2015) onducted experiments on the lift resistance of T-foil in a water tunnel at different flow rates and attack angles; the results confirmed a strong agreement between experimentally measured lift coefficients and theoretical values derived from a combination of a static lift curve slope and

Article Highlights

- A ride control system consisting of dual T-foils is proposed to generate a larger righting moment than a common single T-foil system.
- The optimal control signal was determined by comparing the pitch responses, heave responses, bow accelerations, and stern accelerations of a vessel in regular waves.
- The effectiveness of various control strategies—namely passive control, linear control, and step control—was investigated to identify the approach that yields the best motion-reduction effect.

✉ Zhi Zong
zongzhi@fyust.edu.cn

[1] School of Naval Architecture, Dalian University of Technology, Dalian, Liaoning 116024, China

[2] CSSC Systems Engineering Research Institute, Beijing 100036, China

[3] School of Vehicles and Inteliggent Transportation, Fuyao University of Science and Technology, Fuzhou, Fujian 350000, China

Theodorsen theory for unsteady lift. AlaviMehr et al. experimentally investigated the performance of an active-center bow-mounted T-foil equipped with a smoothness control system based on a 2.5 m catamaran model (Lavroff et al., 2009; Lavroff et al., 2013). Their findings indicated that when the T-foil flapped at an angle of 15°, the model sunk approximately 7 mm, confirming its effectiveness in generating vertical force (AlaviMehr et al., 2016). To set the RCS gains for a control strategy, a T-foil and stern spoilers were utilized to excite only pitch or heave motion in a model. A proposed nonlinear control method was employed to manage RCSs (AlaviMehr et al., 2017). which consistently used maximum configuration to effectively control vessel motion and considerably improve RCSs' performance. Furthermore, how this control strategy affected kinematics during water entry impulses and energy transfer acting upon catamaran models was examined (AlaviMehr et al., 2019). Results demonstrated that RCSs substantially reduced entry impulse and total strain energy.

Comprehensive studies on T-foil have been conducted. Zong et al. (2019) investigated the motion-suppression performance of an actively controlled T-foil on a trimaran and found that compared with passive control, an actively controlled T-foil can considerably improve the suppression of heave amplitude and pitch angle. Additionally, Ticherfatine et al. (Ticherfatine and Qidan, 2018; Ticherfatine and Zhu, 2018). confirmed that their proposed iPD controller is more effective than a PD controller in eliminating fluctuating disturbances affecting T-foils; this new controller can continuously re-identify system dynamics and enhance dynamic behavior. Furthermore, Liu et al. (2021) successfully decoupled T-foils and flaps and designed a trimaran motion derolling reduction controller based on the concept of Kalman filter combined forces and moments; the experimental results verified the controller's attachment effectiveness and efficiency. Jiang et al. (2020) proposed a hybrid control method to regulate the behavior of a T-foil, demonstrating that it can regulate linear and step control and considerably reduce vertical motion. Rozhdestvensky and Htet (2021). proposed a mathematical model with wing devices that use ocean waves as renewable energy sources; the model helps to estimate the seaworthiness of ships with wing installations during the design process to explore options for directional influences on ship heave and pitch movements and to moderate these movements and correspondingly reduce additional wave drag. Yang et al. (2019) used an overlapping grid to simulate an advanced catamaran fitted with an active T-foil under each bow. Compared with EFD data, the results are in good agreement, showing the feasibility and effectiveness of the method in simulating the hydrodynamics of ships with active appendages.

In addition to the utilization of a single T-foil, the use of dual T-foils has been proposed and numerically investigated. Cakici et al. (2018) proposed equipping a motor yacht with bow and stern T-foils to evaluate the performance of a static output feedback controller in reducing vertical acceleration. Simulation results indicate considerable reductions in pitch motion, bow vertical acceleration, and stern vertical acceleration. Kucukdemiral et al. (2019) conducted a numerical investigation into the model predictive controller for mitigating the vertical motion of passenger ships under irregular wave excitation. The design considers actuator amplitude and rate saturation phenomena, and a pair of active stabilizing fins mounted on the bow and stern were used for the ship's motion control system. By applying MPC-based discrete controllers, numerous simulation studies have considerably reduced vertical acceleration at various positions along the ship, including the bow, center, and stern.

The aim of this study is to investigate the motion-reduction performance of a dual T-foil system on a high-speed monohull. A DTMB5415 ship model was constructed, which was equipped with two T-foils positioned at the bow and stern of the vessel. A dual T-foil control system was proposed and tested under regular wave conditions. The effects of different control signals were initially compared, and three distinct control strategies applied to the system were assessed: passive, linear, and step control. The aim was to compare their motion-reduction performance.

1.2 Outline

The paper is structured as follows. Section 2 describes the experimental setup and the T-foil geometry. Section 3 introduces the T-foil control unit and the control method. Section 4 presents the analysis of experimental data of different control signals and strategies and discusses the effect of the dual T-foil system on the drag of the ship model. Finally, in section 5, conclusions regarding the outcome of this study are presented.

2 Experimental setup

2.1 Test model

The experiment was conducted in the Towing Tank of Dalian University of Technology. The test object is the DTMB5415 ship model, and the scale-down ratio of the model is 1∶30. The model, which ensures geometric similarity to a real ship, is made of wooden material processed with sufficient stiffness. The center of gravity position and mass moment of inertia of the model and the real ship have a similar relationship to the relationship of a real ship. The ship model for this test is shown in Figure 1, and the main parameters of the real ship and the model are given in Table 1.

Figure 1 DTMB 5415 Ship model

Table 1 Main parameters and ship form parameters

Main parameters	Real ship	5415 model
Length between vertical lines (m)	142.000	4.733 0
Design waterline length (m)	142.170	4.739 0
Design waterline width (m)	19.050	0.635 0
Design draught (m)	6.150	0.205 0
Drainage capacity (m^3)	8 584.785	0.310 2
Square factor	0.507	0.507 0
Model scaling ratio		30∶1

2.2 Active control T-foil

The T-foil structure is depicted in Figure 2, comprising a vertical foil, a fixed horizontal foil, a flap, a trunk and end plates. In Table 2 is provided specific parameters for the T-foil, including a maximum flap angle $(\varphi_{\max})$ of 15°. The upper part of the swing rod connects to the stepmotor slide rail, allowing for precise control of the swinging connecting rod for driving the flap at a specified angle. To reduce additional resistance to the hull, the mechanism at the bottom of the perimeter well and the top of the vertical foil is shaped to fit seamlessly and to have no protruding structure or blunt body. Additionally, transmission devices are completely enveloped within the vertical foil, which reduces contact with the external fluid and further decreases resistance during navigation. This design results in a considerable reduction in fluid drag compared with traditional one-piece oscillating T-foil mechanisms (Polo et al., 2001; AlaviMehr et al., 2015). Furthermore, rectangular end plates can be added to enhance lift for improved performance. In conclusion, this study's T-foil mechanism exhibits a high lift-to-drag ratio.

The dual T-foils are installed on the ship's bottom baseline. The bow T-foil is positioned at 1 470 mm (l_B) from amidships, and the stern T-foil is positioned at 1 400 mm (l_S) from amidships. As illustrated in Figure 3, the G-point is the center of gravity of the ship model.

2.3 Data measurement methods and expression of results

In this study, various test data, such as pitch, heave, and navigational resistance, need to be measured in the ship model test. The primary measurement instrument utilized

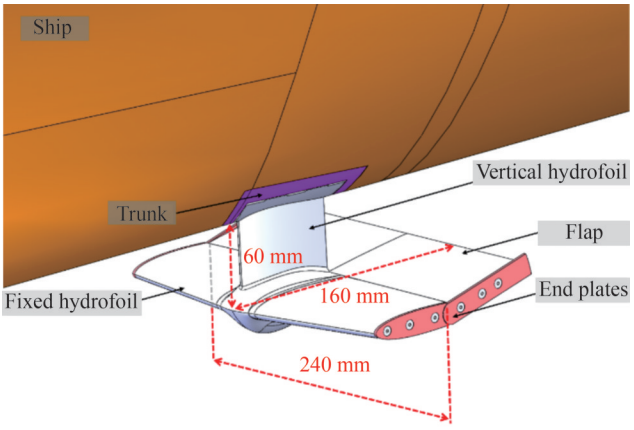

Figure 2 T-foil structure chart

Table 2 T-foil parameters

Index	Model values
Airfoil shape	NACA0012
Wingspan	240 mm
Chord length	160 mm
Maximum angle	±15°
Vertical foil height	60 mm

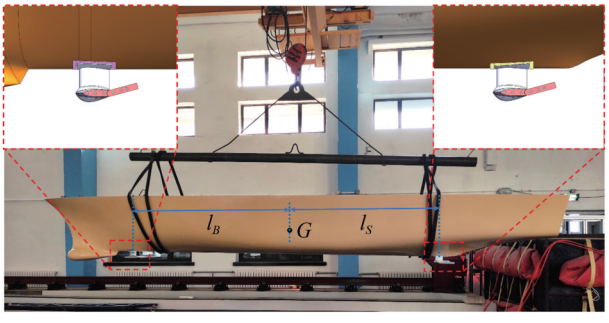

Figure 3 Side view of the model

for collecting these data is a six-degree-of-freedom seaworthy instrument (Figure 4), which is mounted on a trailer to drive the model and measure its motion. Furthermore, these motion parameters can be acquired with a gyroscope, and an accelerometer is employed to measure the head-to-stern acceleration of the model.

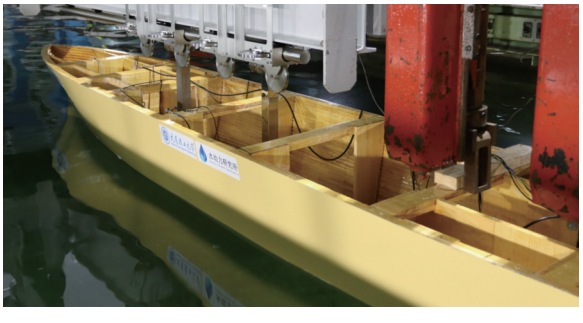

Figure 4 Wave resistance test equipment

The dimensionless responses of the heave and pitch are defined in the following form:

$$y^* = \frac{y}{\zeta} \tag{1}$$

$$\gamma^* = \frac{\gamma \cdot L}{2 \cdot \pi \cdot \zeta} \tag{2}$$

The dimensionless local acceleration is

$$b^* = \frac{\ddot{y}_b}{g} \tag{3}$$

Then the resistance coefficient is given by

$$C_r = \frac{R}{\frac{1}{2}\rho U^2 S} \tag{4}$$

3 T-foil control method

3.1 Dual T-foil control system

The dual T-foil control system primarily comprises a control unit, an altitude sensor, an actuator, and upper computer software. The control unit (Figure 5) is a miniature control board that receives and processes signals from the altitude sensor to regulate the rotation of the stepmotor. The altitude sensor consists of three single-axis accelerometers and three single-axis gyros to measure the angular velocity, accelerations in 3D space, and inclination values. The actuator employs a stepmotor to drive the slide rail and precisely adjust the flap angle of the T-foil by controlling the rotation angle of the stepmotor. Additionally, the upper computer software records real-time sensor data and provides a storage function for easy post-test analysis. Figure 8 provides the details of the dual T-foil control strategy.

During tests, the altitude sensor is mounted on the model. Heave velocities, pitch velocities, and pitch values are transmitted to the micro-control board, which then computes the real-time flap angle φ (Figure 6) and directs the stepmotor to adjust the flap angle φ accordingly. Notably, the bow and stern flap angles have equal magnitudes but opposite directions. In the seakeeping tests, the actuator maneuvers the flap to rotate at a corresponding angle in order to generate damping force, thus preventing pitch motion.

3.2 Dual T-foil control strategy

3.2.1 Passive control strategy

The passive control of dual T-foils maintains the fixed angle of the T-foil flap at $\varphi_{\text{fixed}} = 0°$.

3.2.2 Linear control strategy

In the linear active control of the dual T-foils, the vertical force and pitching moment generated are linearly related to the control signal. This setup allows for the continuous adjustment of the flap angle in real time, thereby enabling the real-time control of the moment generated by the dual T-foils. The various control signals are collectively referred to as S. At the onset of ship motion, passive control is initially employed, and monitoring is conducted on the maximum value $\left(S_{\max}\right)$, minimum value $\left(S_{\min}\right)$, and amplitude $\left(S_a\right)$ of S. The maximum and minimum values correspond to the respective flap angles of $\pm\varphi_{\max}$. Once active control begins, the linear control equation for flap angle is given by

$$\varphi_L = \varphi_{\max}\frac{S}{S_a},\ -\varphi_{\max} \leqslant \varphi_L \leqslant \varphi_{\max} \tag{5}$$

3.2.3 Step control strategy

In the step control strategy, a change in the direction of a control signal triggers an immediate adjustment of the flap angle to its maximum speed. Throughout this process, dual T-foils are consistently controlled with a flap angle $\varphi_S = \pm\varphi_{\max}$.

4 Results and discussion

4.1 Comparison of control signals

To investigate the effect of the control signals on the stabilizing efficiency of the dual T-foils in the same control strategy, a step control strategy was employed to compare the pitch velocity signals with the bow motion velocity signals. During the comparison test, a model speed of 2.792 m/s was selected to correspond to a real ship speed of 30 knots. Wavelengths of 3.75, 5, 6.25, 7.5, 8.75, and 10 m were tested. Variations in the amplitudes of pitch, bow accelera-

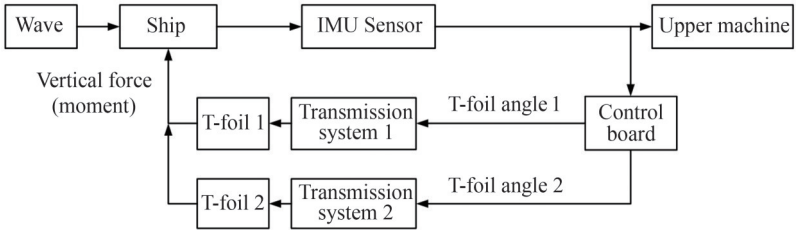

Figure 5 Dual T-foil control strategy

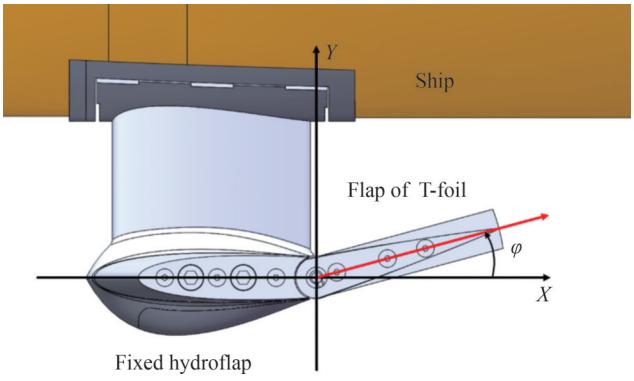

Figure 6 T-foil swing angle diagram

tions, stern accelerations, and heave motion response with encounter frequency are depicted in Figures 7–10 for analysis and discussion purposes.

Figure 7 demonstrates that control signals can effectively reduce the pitch of the ship. Notably, the stabilizing efficiency of the pitch velocity signal surpasses that of the local velocity signal across a wide range of encounter frequencies. A similar trend is evident in bow acceleration motion (Figure 8) and stern acceleration motion (Figure 9). Active control has minimal influence on the heave (Figure 10) primarily because the vertical forces generated by the bow and stern T-foil are equal but opposite in direction and effectively cancel each other out.

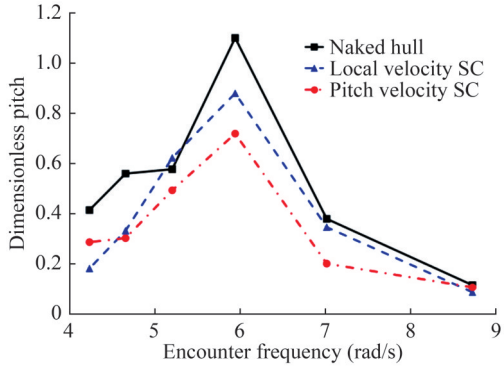

Figure 7 Pitch amplitude response for different control signals

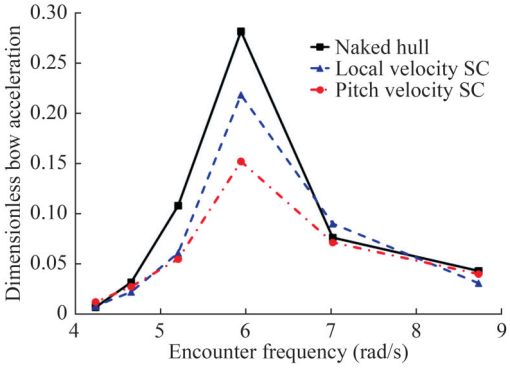

Figure 8 Amplitude response of bow acceleration for different control signals

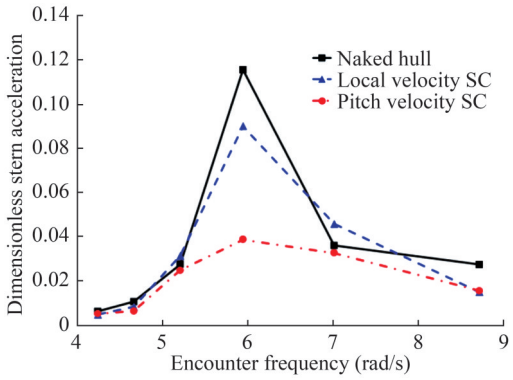

Figure 9 Amplitude response of stern

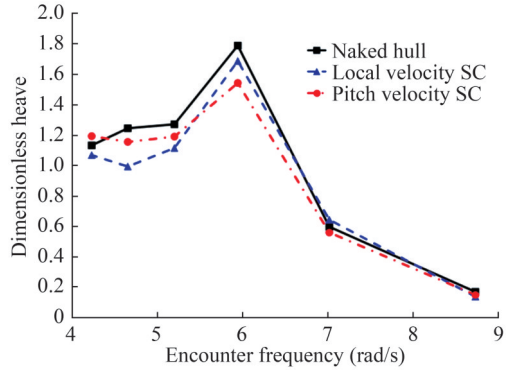

Figure 10 Heave amplitude response for different control signals

To further analyze the rolling reduction of the dual T-foil device on the hull, this study extracts and analyzes the time history data of hull pitch under different working conditions. Figure 11 displays the five-second data of pitch in the experimental stability stage at an encounter frequency of 5.95 rad/s. The active control T-foils demonstrate a noticeable stabilizing effect under both control signal conditions. Additionally, in both cases, the T-foils have a clear stabilizing effect on bow-lifting motion. Furthermore, compared with using bow motion speed as the control signal, utilizing pitch angular velocity as an input signal increases stability. Therefore, in selecting a control strategy, we opted to utilize the pitch velocity signal for dual T-foil control.

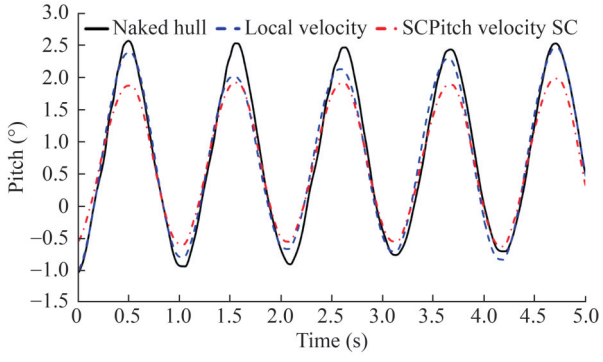

Figure 11 Pitch time history for various control signals

4.2 Comparison of control strategies

To investigate the effects of control strategies on the performance of the dual T-foils, an experiment was conducted using passive control, linear control, and step control to stabilize the ship's motion. The control signal used was pitch velocity. Figure 12 illustrates that heave response amplitude varies with encounter frequency. When active T-foil control is applied at each encounter frequency, the heave response of the ship closely resembles that of a naked hull. This finding indicates that the dual T-foils have minimal effects on the heave motion of the ship. During the control process involving dual T-foils, real-time monitoring reveals that the flap swing directions of both T-foils are opposite to each other and result in equal but opposite lift moments exerted on the ship. These opposing lifts neutralize each other and thus have little impact on heave motion.

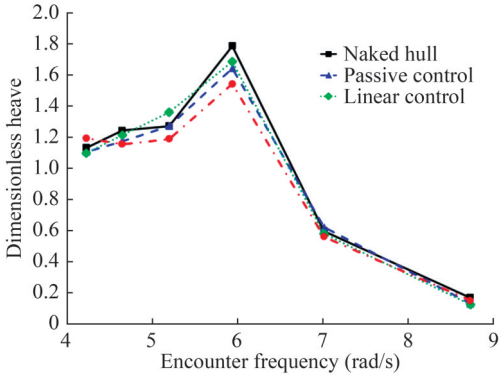

Figure 12 Heave amplitude response with different control strategies

Figure 13 illustrates that pitch amplitude response varies with encounter frequency. The pitch of the ship with passive control T-foil is reduced by 22.19% at its peak, compared with the naked hull. Additionally, the stabilizing efficiency of linear control is similar to that of passive control. Notably, considerable improvement in stabilizing efficiency is achieved with the dual T-foils using step control, which can reach 34.52% at its peak, which is approximately 12% higher than that of passive control. The motion reduction effect of step control surpasses that of linear and passive controls. Figure 14 displays the time history data of pitch angles under various working conditions at an encounter frequency of 6. The rolling reduction effects of different control strategies remain stable. The rolling reduction effect of different working conditions is similar when the ship is raised. However, when the ship is buried, the step control strategy demonstrates the most effective stability effect. In summary, step control yields the best effect at an encounter frequency of 5.95 rad/s.

To investigate the local motion of the ship under different control strategies, measurements were performed on the basis of the response of bow and stern accelerations.

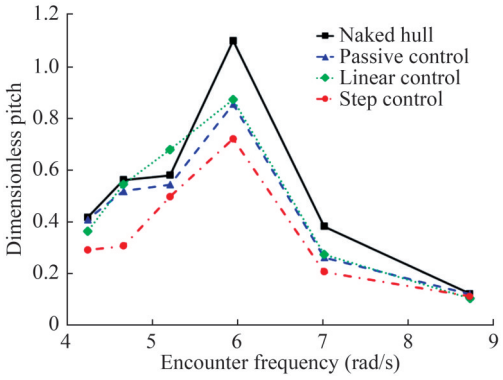

Figure 13 Pitch amplitude response with different control strategies

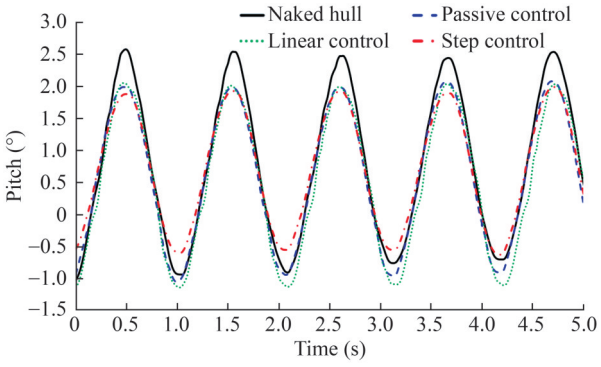

Figure 14 Pitch time history for different control strategies

Bow acceleration response varies with encounter frequency (Figure 15). Overall, step control showed the most effective rolling reduction effect across the full frequency range, followed by linear control. At an encounter frequency of 5.95 rad/s, the naked hull exhibited the largest amplitude of bow motion acceleration. At the same frequency, the dual T-foils demonstrated a clear rolling reduction effect. The motion reduction effect of step control compared with the naked hull was 45.89%, which was 24% higher than that of the passive control. The amplitude of stern acceleration with encounter frequency was similar to bow motion acceleration (Figure 16). Step control had the best rolling reduction effect across all frequencies for stern motion acceleration. Notably, at an encounter frequency of 5.95 rad/s, the maximum motion reduction effect achieved by step control relative to the bareboat was 66.52%.

For the active control system of the dual T-foils, step control has the most stabilizing effect on vertical motion, effectively reducing motion across all frequencies. Experimental results show that the step control system of the dual T-foils considerably reduces motion across the entire frequency band. At an encounter frequency of 5.95 rad/s, the dual T-foils notably mitigate rocking effects. Figures 17 and 18, respectively, illustrate maximum vertical motion without T-foil and under the condition of step control with dual T-foils. The rolling reduction effect of the dual T-foils is clearly evident in these figures.

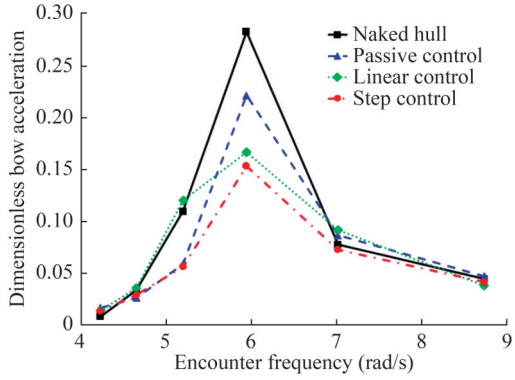

Figure 15 Amplitude response of bow acceleration for different control strategies

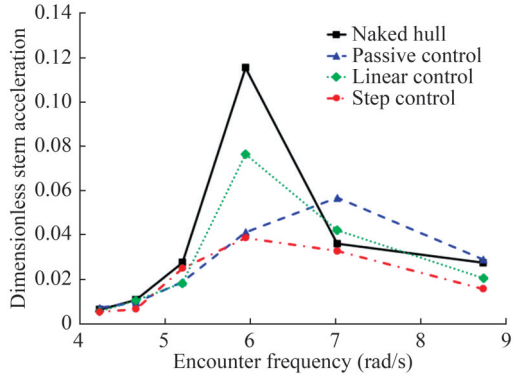

Figure 16 Amplitude response of stern acceleration for different control strategies

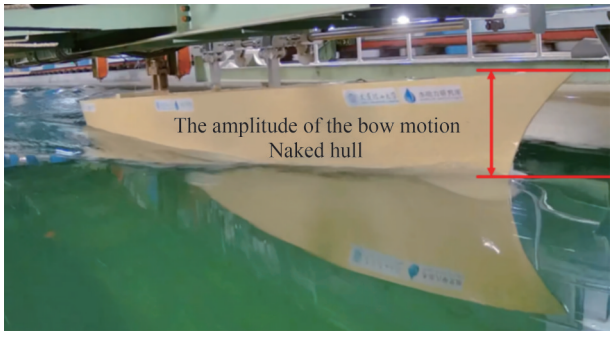

Figure 17 Maximum vertical motion without T-foil

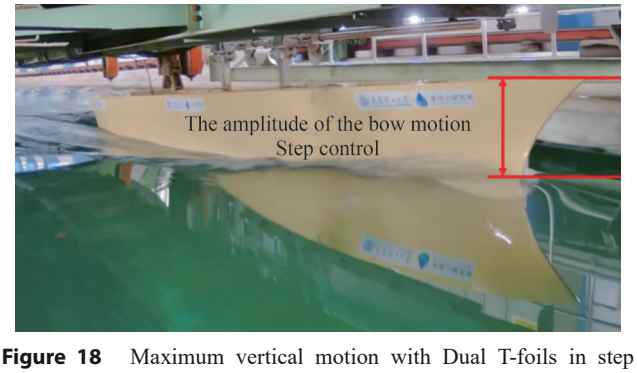

Figure 18 Maximum vertical motion with Dual T-foils in step control

4.3 Drag effects of the dual T-foil system

To investigate the impact of dual T-foils on the sailing resistance of a ship, we conducted measurements of the ship's sailing resistance in various states: naked hull, passive control, linear control, and step control. These measurements were obtained at a speed of 2.792 m/s. The average values of the ship's resistance under different encounter frequencies are presented in Figure 19. A small increase in resistance was observed for all three control strategies and is approximately 10% of the resistance of the naked hull state. Additionally, resistance from active control compared with passive control increases from 5% to 10%. The effect of dual T-foils on the navigation resistance of ships is extremely small.

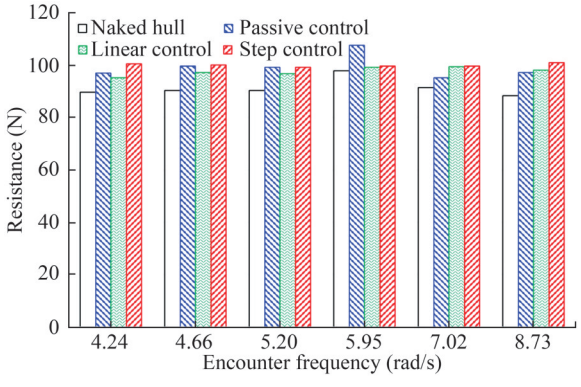

Figure 19 Resistance average versus encounter frequency curve

5 Conclusions

The dual T-foil system was proposed, and a DTMB5415 ship model experiment was conducted to evaluate the effectiveness of the system in reducing pitch motion. The main conclusions of this study are as follows:

1) Compared with different control signals with a step control strategy, the pitch velocity control signal demonstrated excellent motion reduction effects under various encounter frequency conditions.

2) Compared with the ship's motion response with different control strategies revealed that step control had the most stable effects across the entire frequency range. The dual T-foils with the step control achieved a peak stabilizing efficiency of 34.52%, which is approximately 12% higher than that achieved by passive control.

3) In different active control strategies, an overall increase of nearly 10% in hull resistance was observed after the installation of the dual T-foil system.

Only regular head waves were used with the DTMB5415 model. Future studies should include experiments using irregular waves. Additionally, time lag reduced motion reduction effectiveness when control was based on data

after changes in ship attitude. Thus, the research team will focus on enhancing predictive capabilities to effectively stabilize and control ship altitude at subsequent moments.

Nomenclature

U	velocity of the ship
Fr	Froude number based on hull waterline length
ρ	Density of water
ζ	amplitude of the wave
l_B	distance from the center of the hull bottom to the bow T-foil
l_S	distance from the center of the hull bottom to the stern T-foil
φ	flap angle of the T-foil (radian, positive bow on)
R	Resistance of ship
y	instantaneous model heave at the longitudinal center of gravity (positive up)
y_b	instantaneous model heave at the site where T-foil was installed (positive up)
$\dot{y}_b$	instantaneous heave velocity at the site where the T-foil was installed (positive up)
$\ddot{y}_b$	instantaneous heave acceleration at the site where the T-foil was installed (positive up)
γ	instantaneous model pitch about the longitudinal center of gravity (radian, positive bow down)
S	wetted surface
C_r	Resistance coefficient
ω_e	wave encounter frequency (rad/s)
L	length of the ship
B	beam of the ship
t	draught of the ship
∇	drainage volume
C_B	block coefficient
y^*	normalized heave amplitude
γ^*	normalized pitch amplitude
b^*	normalized local acceleration amplitude

Funding This work was supported by Shenzhen 2022 Key Project for Technological Research (Grant Number JSGG202208311108 03006), key technology research and demonstration project of 10 MW deep-sea floating offshore wind turbine (DTGD-2023-10174), and key technology research task of floating offshore combined wind and wave power generation and MIIT program for Floating VAWT.

Competing interest Yichen Jiang and Guiyong Zhang are editorial board member for the Journal of Marine Science and Application and was not involved in the editorial review, or the decision to publish this article. All authors declare that there are no other competing interests.

References

Aranda J, Díaz JM, Ruipérez P, Rueda TM, López E (2001) Decreasing of the motion sickness incidence by a multivariable classic control for a high speed ferry. IFAC Proceedings Volumes 34(7): 273-278. https://doi.org/10.1016/s1474-6670(17)35095-4

AlaviMehr J, Davis MR, Lavroff J (2015) Low reynolds number performance of a model scale T-foil. International Journal of Maritime Engineering 157(A3): 175-188. https://doi.org/10.3940/rina.ijme.2015.a3.336

AlaviMehr J, Davis MR, Lavroff J, Holloway DS, Thomas GA (2016) Response of a high-speed wave-piercing catamaran to an active ride control system. International Journal of Maritime Engineering 158(A4): A325-A335. https://doi.org/10.5750/ijme.v158ia4.1002

AlaviMehr J, Lavroff J, Davis MR, Holloway D, Thomas G (2017) An experimental investigation of ride control methods for high-speed catamarans Part 1: reduction of ship motions. Journal of Ship Research 61: 35-49. https://doi.org/10.5957/josr.61.1.160041

AlaviMehr J, Lavroff J, Davis MR, Holloway D, Thomas G (2019) An experimental investigation on slamming kinematics, impulse and energy transfer for high-speed catamarans equipped with ride control systems. Ocean Engineering 178: 410-422. https://doi.org/10.1016/j.oceaneng.2019.02.004

Cakici F, Yazici H, Alkan AD (2018) Optimal control design for reducing vertical acceleration of a motor yacht form. Ocean Engineering 169: 636-650. https://doi.org/10.1016/j.oceaneng.2018.10.006

Davis MR, Hollway DS (2003) Motion and passenger discomfort on high speed catamarans in oblique seas. International Shipbuilding Progress 50(4): 333-370. https://doi.org/10.3940/rina.ijme.2003.a4.333

Esteban S, Cruz JMDL, Giron-Sierra JM, Andres BD, Díaz JM, Aranda J (2000) Fast ferry vertical accelerations reduction with active flaps and T-foil. IFAC Proceedings Volumes 33(21): 227-232. https://doi.org/10.1016/s1474-6670(17)37079-9

Esteban S, Andres BD, Giron-Sierra JM, Polo OR (2001) A simulation tool for a fast ferry control design. IFAC Proceedings Volumes 34(7): 267-272. https://doi.org/10.1016/s1474-6670(17)35094-2

Esteban S, Andrés-Toro B, Besada-Portas E, Girón-Sierra JM, Cruz JMDL (2002) Multiobjective control of flaps and T-foil in high-speed ships. IFAC Proceedings Volumes 35(1): 313-318. https://doi.org/10.3182/20020721-6-es-1901.01277

Esteban S, Giron-Sierra JM, Andres-Toro BD, Cruz JMDL, Riola JM (2005) Fast ships models for seakeeping improvement studies using flaps and T-foil. Mathematical and Computer Modelling 41(1): 1-24. https://doi.org/10.1016/j.mcm.2004.09.002

Fang CC, Chan HS (2007) An investigation on the vertical motion sickness characteristics of a high-speed catamaran ferry. Ocean Engineering 34(14-15): 1909-1917. https://doi.org/10.1016/j.oceaneng.2007.04.001

Giron-Sierra JM, Esteban S, Andres BD, Diaz JM, Riola JM (2001) Experimental study of controlled flaps and T-foil for comfort improvement of a fast ferry. IFAC Proceedings Volumes 34(7): 261-266. https://doi.org/10.1016/s1474-6670(17)35093-0

Giron-Sierra JM, Katebi R, Cruz JMDL, Esteban S (2002) The control of specific actuators for fast ferry vertical motion damping. International Conference on Control Applications IEEE, Glasgow, UK, 2002: 304-309. https://doi.org/10.1109/cca.2002.1040203

Gopinath S, Vijayakumar R (2023) Computational analysis of the effect of hull vane on hydrodynamic performance of a medium-speed vessel. Journal of Marine Science and Application 22: 762-774. https://doi.org/10.1007/s11804-023-00378-y

Hollway DS, Davis MR (2006) Ship motion computations using a high froude number time domain strip theory. Journal of ship

research 50: 15-30. https://doi.org/10.5957/jsr.2006.50.1.15

Jacobi G, Thomas G, Davis M, Holloway D, Davidson G, Roberts T (2012) Full scale motions of a large high-speed catamaran: the influence of wave environment, speed and ride control system. The International Journal of Maritime Engineering 154: A143-A155. https://doi.org/10.3940/rina.ijme.2012.a3.238

Jiang YC, Bai JY, Sun Y, Sun YF, Zong Z (2020) Numerical investigation of T-foil hybrid control strategy for ship motion reduction in head seas. Ocean Engineering 217: 107924. https://doi.org/10.1016/j.oceaneng.2020.107924

Kucukdemiral IB, Cakici F, Yazici H (2019) A model predictive vertical motion control of a passenger ship. Ocean Engineering 186: 106100. https://doi.org/10.1016/j.oceaneng.2019.06.005

Lavroff J, Davis MR, Holloway DS, Thomas G (2009) The vibratory response of high-speed catamarans to slamming investigated by hydroelastic segmented model experiments. International Journal of Maritime Engineering 151: 1-11. https://doi.org/10.3940/rina.ijme.2009.a3.159

Lavroff J, Davis MR, Holloway DS, Thomas G (2013) Wave slamming loads on wave-piercer catamarans operating at high-speed determined by hydro-elastic segmented model experiments. Marine Structures 33: 120-142. https://doi.org/10.1016/j.marstruc.2013.05.001

Liu ZL, Zheng LH, Li GS, Yuan SZ, Yang SB (2021) An experimental study of the vertical stabilization control of a trimaran using an actively controlled T-foil and flap. Ocean Engineering 219: 108224. https://doi.org/10.1016/j.oceaneng.2020.108224

Polo OR, Esteban S, Maron A, Gran L, Cruz JMDL (2001) Control code generator used for control experiments in ship scale model. IFAC Proceedings Volumes 34(7): 279-284. https://doi.org/10.1016/s1474-6670(17)35096-6

Rozhdestvensky KV, Htet ZM (2021) A mathematical model of a ship with wings propelled by waves. Journal of Marine Science and Application 20: 595-620. https://doi.org/10.1007/s11804-021-00221-2

Thomas G, Winkler S, Davis M, Holloway D, Matsubara S, Lavroff J, French B (2011) Slam events of high-speed catamarans in irregular waves. Journal of Marine Science and Technology 16: 8-21. https://doi.org/10.1007/s00773-010-0105-y

Ticherfatine M, Qidan Z (2018) Model-free approach based on intelligent PD controller for vertical motion reduction in fast ferries. Turkish Journal of Electrical Engineering & Computer Sciences 26: 393-406. https://doi.org/10.3906/elk-1703-224

Ticherfatine M, Zhu Q (2018) Fast ferry smoothing motion via intelligent PD controller. Journal of Marine Science and Application 17(2): 273-279. https://doi.org/10.1007/s11804-018-0024-6

Yang D, Shao F, Li C, et al (2019) Overlapping grid technique for numerical simulation of a fast-cruising catamaran fitted with active T-Foils. Journal of Marine Science and Application 18: 176-184. https://doi.org/10.1007/s11804-019-00077-7

Zong Z, Sun YF, Jiang YC (2019) Experimental study of controlled T-foil for vertical acceleration reduction of a trimaran. Journal of Marine Science and Technology 24(2): 553-564. https://doi.org/10.1007/s00773-018-0576-9